JOURNAL OF Applied Polymer SCIENCE

Full Factorial Design-of-Experiments for Preparation of Crosslinked Dextran Microspheres

Hamed Salimi Kenari,[1] Mohammad Imani,[1] Azizollah Nodehi[2]

[1]Department of Novel Drug Delivery Systems, Iran Polymer and Petrochemical Institute, Tehran, Iran

[2]Department of Process Modeling and Control, Iran Polymer and Petrochemical Institute, Tehran, Iran

Correspondence to: M. Imani (E-mail: m.imani@ippi.ac.ir)

ABSTRACT: This work describes full factorial design-of-experiment methodology for exploration of effective parameters on physical properties of dextran microspheres prepared via an inverse emulsion (W/O) technique. Microspheres were prepared by chemical crosslinking of dextran dissolved in internal phase of the emulsion using epichlorohydrin. The input parameters were dextran concentration in the aqueous phase, crosslinking ratio, and concentrations of sodium hydroxide and span 80 as the reaction catalyst and surfactant, respectively. Chemical structure of the resulting microspheres was analyzed spectroscopically using Fourier-transform infrared technique. Final decomposition temperature, mean particle size and its distribution and equilibrium swelling ratio were selected as output responses. Microspheres with smooth surface were obtained according to scanning electron micrographs. It was found that an increase in dextran concentration in the aqueous internal phase increases mean particle diameter of the resulting microspheres, significantly. Moreover, water uptake capacity for the microspheres was dependent on both the dextran concentration and crosslinking ratio. © 2012 Wiley Periodicals, Inc. J. Appl. Polym. Sci. 000: 000–000, 2012

KEYWORDS: microspheres; dextran; crosslinking; inverse emulsion; experimental design

Received 27 August 2011; accepted 29 April 2012; published online
DOI: 10.1002/app.37983

INTRODUCTION

The design and synthesis of functional polymeric hydrogel microspheres is one of the progressive fields due to their biomedical applications. These materials can be used in a wide array of fields from highly effective hemostatic agents in medicine to analytical chemistry as chromatographic stationary phases for size exclusion or enantioselective separation of biomolecules.[1–7] Different synthetic and naturally occurring polymers have been reported in fabrication of these microspheres, however; especial attention is paid to the naturally occurring polysaccharides including alginates, chitosan, dextran, etc., due to their biodegradability and biocompatibility.[8] It is also known that polysaccharides can be easily crosslinked using various functional organic or inorganic chemicals to form hydrogel networks capable of entrapping high quantities of water into their structure.[9]

Dextran as a polysaccharide possesses a complex glucan structure of nearly 5–10% (1,3) α-linked branched units, on average; along with its major linear backbone composed of (1,6) α-D-glycoside residues derived from bacterial sources having three hydroxyl functional groups per each glucose moiety. Dextran is a hydrophilic, biocompatible, water-soluble, and inert biopolymer which does not affect cell viability in biological systems hence it owes a long history of application as blood plasma expander, carrier system for a variety of therapeutic agents and hemostatic agent for many years.[4,10]

Inverse emulsion (W/O) crosslinking of aqueous polysaccharide solutions is frequently reported for preparation of hydrogel microspheres.[11–17] Crosslinking of the biopolymer can be achieved via chemical reactions to produce permanent covalent bonds employing different crosslinking agents like diisocyanates, glutaraldehyde, and epichlorohydrin (ECH). Application of ECH in crosslinking of polysaccharides has been studied by Guner et al.[18] and Atyabi et al.[19] However, limited information is available on its effect on the finally achieved characteristics of the microspheres. The characteristics such as particle size and its distribution not only can be affected by molecular characteristics of the polymers, e.g., molecular weight distribution or being linear or branched but also by kinetics and processing conditions, e.g., internal phase viscosity, interfacial tension, catalyst, and crosslinking extent as can be expected by theoretical descriptions presented by Pacek,[20] Bahukudumbi,[21] or Berchane.[22] Considering the previous history of polysaccharides

application, there has been no report in the literature on the effects of the influential parameters governing inverse emulsification crosslinking technique on the final microspheres characteristics at the best of our knowledge.

In this study, crosslinked dextran microspheres (CDMs) were synthesized by crosslinking of dextran dissolved in internal phase of an inverse emulsion system (W/O) using ECH as a crosslinking agent. An experimental design based on full factorial methodology was adopted to look for the effective formulation variables on the targeted responses. The effects of four key parameters including dextran concentration, crosslinking ratio, and concentrations of catalyst, i.e., sodium hydroxide (NaOH), and surfactant (Span® 80) were investigated on the final properties of the resulting microspheres such as mean particle size and its distribution, and swelling ratio. The model was fitted by carrying out multiple regression analysis and *F*-statistics to identify statistically significant terms. Structure and properties of the CDMs were studied by optical reflectance microscopy, scanning electron microscopy (SEM), Fourier-transform infrared (FTIR) spectroscopy, and thermogravimetric analysis (TGA) techniques.

MATERIALS AND METHODS

Materials

USP grade dextran 70 ($\overline{M}_n$ = 45,040 g mol^{-1}, polydispersity index = 1.47) was purchased from Pharmacosmos A/S (Holbaek, Denmark). All chemicals including ECH, *n*-octane, NaOH, and sorbitan monooleate (Span® 80, hydrophilic-lipophilic balance = 4.7) were of analytical grade and used as supplied by Merck Chemicals (Darmstadt, Germany). Deionized water (high performance liquid chromatography grade) was prepared in house using reverse osmosis technique (AquaMax 311, YoungLin Instruments, Anyang, South Korea) and used in preparation of solutions also microspheres work-up.

Preparation of Crosslinked Dextran Microspheres

Inverse emulsion crosslinking technique was adopted from Hamdi et al.,[23] with some modifications. In a typical batch, the organic continuous phase was consisted of 245 mL of *n*-octane containing 2% W/V of the surfactant. Continuous phase was charged in a 400-mL three-necked glass reaction vessel equipped with a thermal jacket, an overhead stirrer (RZR 2102, Heidolph Instruments, Schwabach, Germany) with a curved blade impeller (three blades, D = 43 mm, and blade angle = 6°), and connected to a syringe pump (Pilot A2, Fresenius Kabi, Germany) for dripping of the reagents. The reaction temperature was controlled at 40°C using a thermostatic bath (Polystat CC3, Huber, Offenburg, Germany). The aqueous phase was prepared by dissolving 6.24 g of dextran (25% W/V) in 20 mL of 1*M* NaOH solution, then homogenized for 5 min at 3000 rpm using a dual centrifugal mixer (SpeedMixer® DAC 150, Hauschild Engineering, Germany) until complete dissolution. Upon charging into the reactor, the aqueous phase was pre-emulsified by stirring at 1300 rpm for 15 min to form a W/O emulsion and assure complete adsorption of surfactant on the surface of droplets. Then the mixing rate was set at 400 rpm on addition of ECH up to the reaction end.

Further on, a corresponding amount of ECH, e.g., 2.1 mL as determined by experimental design was added dropwise to the reaction vessel using a syringe pump at a rate of 4 mLh^{-1}. The reaction flask was left to be stirred overnight for an additional 18 h to assure complete reaction. The resulting microspheres were separated from the reaction mixture by filtration on Whatman filter paper (No. 42, Whatman, Brentford, UK) then washed twice with *n*-octane and distilled water, sequentially. Finally, microspheres were subjected to solvent exchange using acetone and/or ethanol and dried *in vacuo*. Schematic representation of the process is shown in Figure 1.

Network Characterizations

The FTIR spectroscopy was accomplished quantitatively on the CDMs to identify its crosslinked structure. To this end, a definite weight of the dried microspheres were thoroughly mixed with KBr using a mortar and pestle and pressed into disks. Spectral scanning was done using an Equinox 55 spectrophotometer (Bruker, Germany) in the range between 400 and 4000 cm^{-1} at 4 cm^{-1} resolution and 16 scans at room temperature.

Equilibrium swelling ratio (ESR) were determined for CDMs by complete immersion of representative samples (n = 6) taken from each batch in distilled water for 3 days at ambient conditions. Sol fractions of the batches were previously extracted during postfabrication work up; however, swelling medium was replaced each day and refurnished with distilled water. The surface water on the bulk of CDM hydrogels was blotted using filter paper then weighed accurately. ESR of CDMs was determined gravimetrically using the following equation:

$$\mathrm{ESR} = [(W_1 - W_0)/W_0] \tag{1}$$

where, W_0 and W_1 are dry (initial) and swollen weights of the samples, respectively.

Average molecular weight between crosslinks ($\bar{M}_C$) was determined according to the model of Flory and Rehner[24] modified by Peppas et al.,[25] for gels in which the crosslinks are introduced in solution:

$$\frac{1}{\overline{M}_c} = \frac{2}{\overline{M}_n} - \frac{\left[\left(\frac{v}{V_1}\right)\left(\ln(1-v_{2,s}) + v_{2,s} + \chi v_{2,s}^2\right)\right]}{v_{2,r}\left[\left(v_{2,s}/v_{2,r}\right)^{1/3} - 2/\varphi\left(v_{2,s}/v_{2,r}\right)\right]} \tag{2}$$

In this equation, $\overline{M}_n$ stands for number-average molecular weight of dextran, V_1 is the molar volume of water (18 cm^3 g^{-1}), v is the partial specific volume of dextran (0.62 cm^3 g^{-1}),[26] χ is the Flory–Huggins interaction parameter between polymer and water (0.473),[27] φ stands for the functionality of crosslinking agent, and $v_{2,r}$ is the polymer volume fraction in the hydrogel immediately after crosslinking but before swelling, which is equivalent to the volume concentration of the solution where crosslinking occurs. The swollen state fraction, $v_{2,s}$, refers to the polymer volume fraction when the hydrogel is fully swollen in the presence of pure water.[27]

The network mesh size (ξ) was calculated for CDMs using the following equation:[29,30]

$$\xi = 0.071(v_{2,s})^{-1/3}\sqrt{\overline{M}_c} \tag{3}$$

The polymer volume fraction at swollen state, $v_{2,s}$, could be mathematically represented by

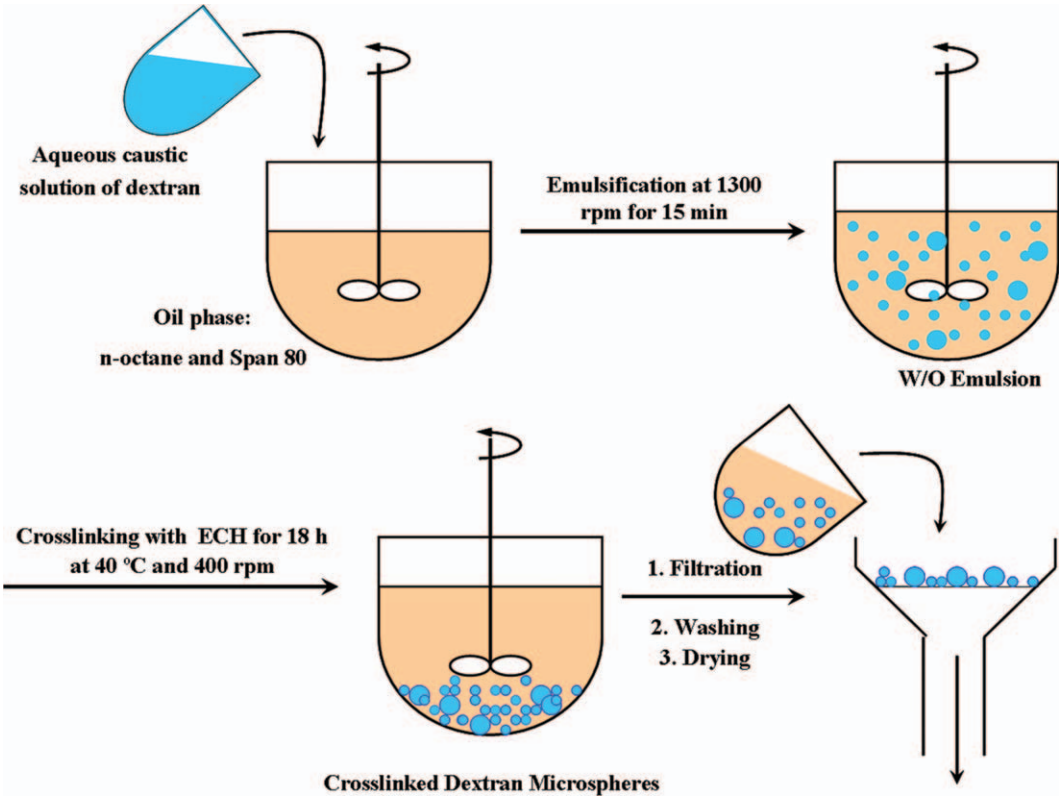

Figure 1. Schematic representation of crosslinked dextran microspheres preparation. [Color figure can be viewed in the online issue, which is available at wileyonlinelibrary.com.]

$$v_{2,s} = \frac{V_p}{V_s} = \frac{W_d/d_p}{[W_d/d_p + (W_s - W_d)/d_w} \quad (4)$$

where, V_p is the volume of polymeric matrix alone, V_s is the volume of the swollen gel, *i.e.*, the total volume of the matrix plus the swelling solvent. W_d is the dried polymer weight, W_s the swollen gel weight, and d_p and d_w are densities of the CDMs at dry state and water, respectively. The density of water was taken as 1 g mL^{-1}.

Thermal Analysis

TGA was carried out using a TGA-PL instrument (Polymer Laboratories, UK) under dynamic nitrogen atmosphere (50 $mLmin^{-1}$) at a heating rate of 10°C min^{-1} and temperature interval between ambient temperatures to complete destruction at 600°C.

Morphology and Particle Size Analysis

Morphology of the CDMs was observed in reflectance mode under a Jenavert optical microscope (Carl Zeiss, Germany). To this end, a small amount of dry microspheres was suspended in purified water (10 mL) and then ultrasonicated for 5 s. A drop of this suspension was placed on a clean glass slide mounted on the stage and observed at different magnifications. Microphotographs were captured using a JVC TK-C1381 color video camera.

Morphology, particle size and its distribution was analyzed using SEM (Vega© Tescan, Czech Republic). Images were analyzed using Microstructure Measurement (version 1.0, Ferdowsi University, Iran) digital image processing software. Samples were mounted on metal stubs and sputter-coated with gold for 4 min before examination. Their internal structure was revealed by cross sectioning the microspheres embedded in an epoxy resin. The Feret's diameter of at least 500 particles was recorded for all batches then volume–surface average particle diameter (D_{32}) was determined using the following equation:[31]

$$D_{32} = \frac{\sum n_i D_i^3}{\sum n_i D_i^2} \quad (5)$$

where, n_i is the number of particles counted of D_i projected area diameter. Uniformity index (UI) was determined using the following formula:

$$UI = D_w/D_n \quad (6)$$

in which D_w and D_n are weight and number average diameters, respectively. D_w and D_n are calculated as follows:[31]

$$D_w = \frac{\sum n_i D_i^4}{\sum n_i D_i^3} 1 D_n = \frac{\sum n_i D_i}{\sum n_i} \quad (7)$$

Experimental Design and Statistical Analysis

A full factorial design-of-experiment (DOE) methodology was adopted using Minitab statistical software (version 15.1, State College, PA) to investigate the effects of selected formulation variables comprising dextran concentration in the aqueous phase (A), NaOH molarity (B), surfactant concentration (C), and crosslinking ratio (D) on the microspheres characteristics. Crosslinking ratio is defined here as the crosslinker to polymer molar ratio. The initial levels for the parameters (Table I) were determined based

Table I. Factors and Factor Levels Investigated According to Full Factorial Experimental Design

		Input parameters as coded values				Experimental responses					
Std. order	Run order	A: Dextran conc. (W/V %)	B: NaOH conc. (*M*)	C: Surfactant conc. (W/V %)	D: Crosslinking ratio (mol mol^{-1})	Equilibrium swelling ratio	$\bar{M}_0$(g mol^{-1})	Mesh size (nm)	Final of thermal decomposition (°C)	Mean particle size (D_{32}, μm)	Uniformity index (UI)
1	1	−1	−1	+1	+1	18.9 ± 1.57	11,515.0	20.19	471	22.30	*1.87*
2	2	−1	+1	+1	+1	13.5 ± 1.34	7213.2	14.37	488	35.81	*1.86*
9	3	−1	−1	−1	−1	16.3 ± 0.87	9543.1	17.53	457	27.44	*1.82*
12	4	+1	+1	+1	−1	8.1 ± 0.84	4921.2	10.15	493	56.73	*2.73*
11	5	+1	−1	−1	−1	6.1 ± 0.39	2814.5	7.09	496	46.94	*2.85*
14	6	−1	+1	+1	−1	17.0 ± 1.81	10,011.2	18.16	490	34.63	*1.73*
3	7	+1	−1	−1	+1	5.9 ± 0.67	2585.6	6.70	514	51.17	*2.12*
4	8	−1	+1	−1	+1	12.6 ± 0.92	5687.0	12.25	501	39.91	*1.26*
5	9	+1	+1	−1	+1	4.2 ± 0.83	1236.2	4.19	528	75.54	*3.11*
6	10	−1	−1	−1	+1	15.5 ± 1.24	8867.9	16.62	492	26.03	*1.57*
7	11	+1	−1	+1	+1	5.4 ± 0.33	2082.3	5.87	499	37.86	*1.7*
16	12	+1	−1	+1	−1	7.2 ± 0.86	11,933.0	19.00	491	39.10	*2.02*
13	13	−1	−1	+1	−1	16.4 ± 1.07	9621.1	17.63	479	25.64	*1.34*
10	14	−1	+1	−1	−1	19.1 ± 1.81	11,536.6	20.24	489	43.24	*1.76*
8	15	+1	+1	+1	+1	6.5 ± 1.08	3273.7	7.74	495	74.54	*2.01*
15	*16*	*+1*	*+1*	*−1*	*−1*	*7.2 ± 0.90*	*3993.9*	*8.84*	*500*	*57.10*	*2.85*

Table II. Formulation and the Results Obtained for Batches According to the Full Factorial Design-of-Experiments

		Levels[a]	
Code	Factor (Unit)	Low	High
A	Dextran concentration (W/V %)	25	50
B	NaOH concentration (*M*)	1	1.5
C	Surfactant concentration (W/V %)	1	2
D	Crosslinking ratio (mol mol^{-1})	150	200

[a]Levels were coded as (−1) and (+1) for low and high levels, respectively.

on the preliminary experiments. Three categories of responses including network characteristics (ESR), final of thermal decomposition temperature (T_f), mean particle diameter, and its distribution were analyzed (Table II). Considering variation of the input parameters in two levels, 16 runs were performed and analyzed according to the design.

The design was analyzed to study the significance of the effects of changing formulation parameters on the final properties of CDMs. Data were reported as mean ± standard deviation at a significance level of $p < 0.05$. A graphical display of the ordered standardized effect of each factor was provided using a Pareto chart, which analyzes the magnitude and the importance of each variable effect. The length of bars in the chart is proportional to the standardized effect. A factor was considered as "statistically significant" if its standardized effect exceeded a threshold. The mean for a given level of a variable is the average of all responses obtained for that level and used for plotting the marginal means. The plot of marginal means provides an important insight into the relationship between a quantitative response variable and the independent variables.

For each response, the respective data were fitted in a factorial equation [eq. (8)] to show the mathematical correlation between the independent and dependent variables as follows:

$$\text{Response} = b_0 + b_1A + b_2B + b_3C + b_4D + b_{12}A * B + b_{13}A * C + \ldots \quad (8)$$

where, b_n is coefficient associated with the factor, n, and the letters, A, B, C. represent the factors in the model. Combinations of factors (such as A^*B) represent an interaction between the individual factors in that term.[32] The coefficients (b_n) were calculated by multiple linear regressions, and the results were analyzed by the software. Here, positive or negative sign of a coefficient shows an increasing or decreasing effect of that specific parameter on the response.

RESULTS AND DISCUSSION

Structural Analysis of the CDMs

The reaction of ECH and soluble polysaccharides under alkaline conditions follows the nucleophilic substitution mechanism known as Williamson synthesis (Figure 2).[33,34] The addition of ECH to dextran chain in the aqueous alkaline medium is a molecular reaction passing via formation of Dex-O^-Na^+ intermediate stage. The fragments formed can be easily transformed to epoxy ring by dehydrochlorination in the presence of NaOH.

FTIR Spectroscopy

Figure 3 shows the FTIR spectra for ECH, dextran, and CDMs obtained in run order 10. All visual results will be reported for this specific run order, just as a representative example, for sake of more consistency. As shown, the signal band appeared at 3418 cm^{-1} of CDMs, which is assigned to the secondary hydroxyl groups, displays a decrease in its intensity in comparison to that of virgin dextran indicating that some secondary hydroxyl groups were consumed during the reaction. In contrast, the peaks at 2919 and 2861 cm^{-1}, attributed to the aliphatic methylene functional groups, showed an increase in their intensities due to the more methylene groups introduced by ECH into the CDMs structure. Appearance of a new absorption band at 1167 cm^{-1}, corresponding to the stretching C—O bands and remarkable decrease in the intensity of epoxy ring at 1269 cm^{-1} (ν stretching), 956 cm^{-1} (C—O stretching), 853 cm^{-1}, and 753 cm^{-1} (C—Cl stretching) supports the formation of new bonds due to the crosslinking reaction.[17,25,35–37]

It should be noted that there could be some side reactions along with the crosslinking reaction, e.g., the reaction of some ECH molecules with only one complementary hydroxyl group of dextran or its reaction with the unreacted pendent epoxy groups. As it is difficult to accurately quantify such side reactions, it is reasonable to assume that the amount of hydroxyl groups from such side reactions is directly proportional to the amount of ECH used in the crosslinking reaction.[38]

Thermal Degradation

TGA thermograms for initial dextran and the resulting CDMs (run order 10, Table II as a representative sample) are illustrated in Figure 4. Table III gives the details of thermal behavior according to the primary and derivative thermograms obtained for both samples. The degradation process of the samples could be divided into two distinct stages. In the first stage, ranged from room temperature to 150°C, weight loss for dextran and CDMs were about 7.5 and 4%, respectively. This weight loss may be due to desorption of moisture as hydrogen-bonded water molecules to the glucose moieties. As well as, this stage perhaps could be ascribed to the elimination of the residual organic solvents used in drying of CDMs.

The degradation process in the second stage can be attributed to the rupture of the main chains of dextran also crosslinking bonds. The onset of thermal degradation is lower for CDMs (i.e., 225 vs. 285 °C) which may be attributed to the different bonds strength between the crosslinked backbone, i.e., dextran chains connected via ether bonds due to the reaction with ECH and intrabackbone covalent bonds.

Weight loss rate for dextran, within a certain range of temperature, was increased rapidly in contrast to what observed for the CDMs, which confirms that these changes are due to dextran crosslinking. This may be attributed to the higher variety of bonds in CDMs comparing with the initial dextran. A significant increase in thermal stability of the microspheres was observed in comparison to the initial dextran especially,

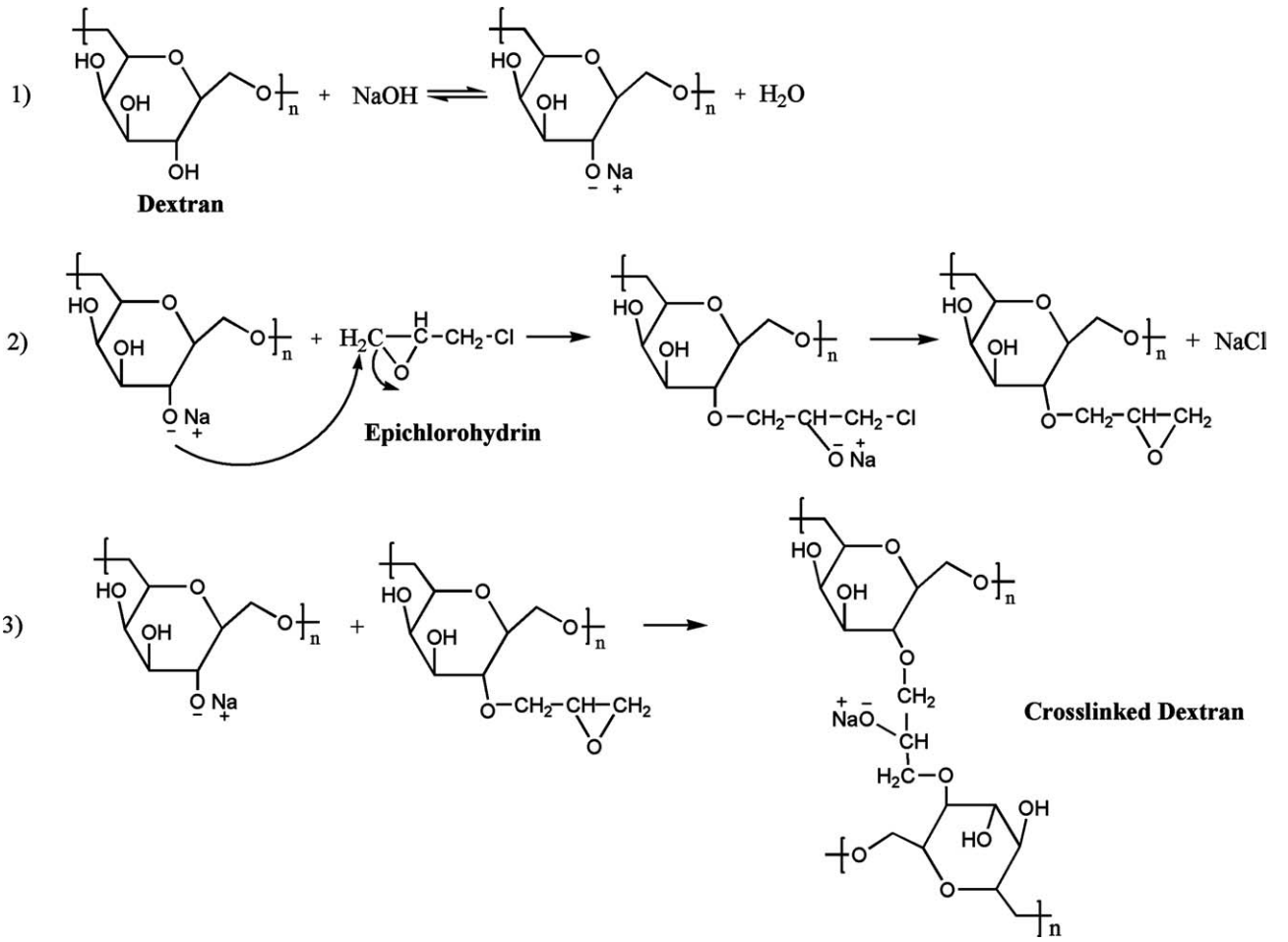

Figure 2. Proposed mechanism for the reaction of ECH with dextran.[32]

considering the remained ash ($T = 600°C$, 26.8% vs. 16.2% for CDMs and dextran, respectively) which is certainly due to its crosslinking and consequent improvement in thermal stability.

Generally, dehydration, depolymerization, and pyrolitic decomposition are involved in thermal degradation in polysaccharides and may be a probable mechanism for the thermal transitions. Accurate assigning of the thermal transitions is a subject of debate.[39] Considering the final degradation temperature, the TGA results clearly indicate that the crosslinking reaction has led in an enhanced thermal stability of CDMs.

Microspheres Morphology

Optical microscopy observations on the dry microspheres [typically shown in Figure 5(a) for run order 10] revealed spherical particles having smooth surfaces with varying mean particle sizes and size distribution between batches. In the swollen state, mean particle sizes were significantly increased depending on degree of equilibrium swelling. The swollen microgels were translucent [Figure 5(b)] as usual in swollen hydrogel microspheres,[40] which can be attributed to the changes in their refractive index on water imbibitions.

Figure 6(a, b) shows SEM micrographs obtained for run order 10. Micrographs reveal predominant perfect spherical architecture for the most CDMs but other morphologies including rough surfaces having microstructure patterns (in submicrometer size) or shrunk ones are also observed. Shrunk faces are especially present in samples prepared using higher concentrations of dextran in the aqueous phase. Most particles showed a moon-face morphology due to the collisions occurred between them that may be regarded as a sign for their tough mechanical properties resulting from a dense, and crosslinked structure.

Cross-sectional micrographs of the particles also showed a uniform architecture [Figure 6(c)]. A border zone (in 3–4 μm thickness) was observed on the particles surface, which may be an indicative of the initiation of the crosslinking reaction from surface of the initial droplets. On formation of a rigid surface layer, the crosslinking reaction inside the droplets will be dominated by a diffusion-controlled mechanism. Hence, the reaction was run overnight to assure complete crosslinking reaction, which was guaranteed by observing a continuous, uniform structure with no pores formed after sol fraction extraction.

Particle Size and Size Distribution of the Microspheres

Mean particle size and the breadth of its distribution are the two key factors significantly affecting critical microspheres properties like water uptake capacity in their final applications like

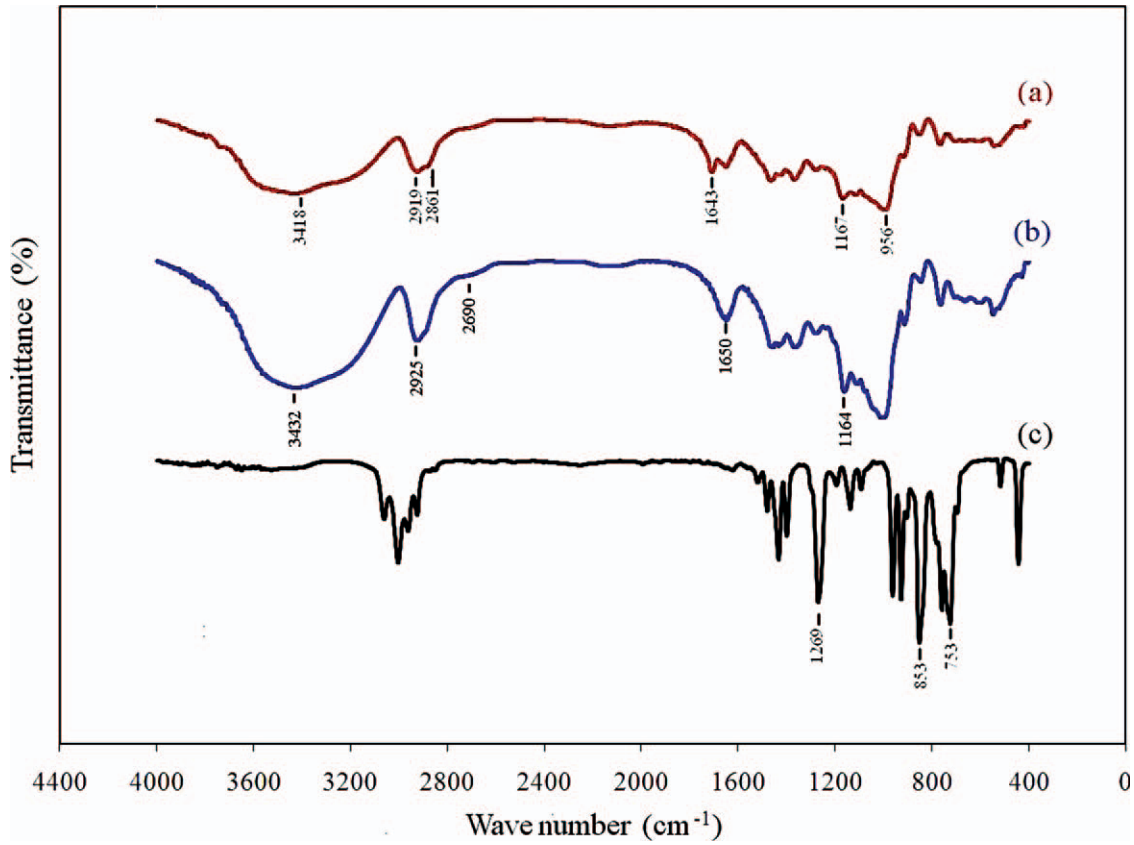

Figure 3. FTIR spectra of (a) crosslinked dextran microspheres, (b) initial dextran, and (c) ECH. [Color figure can be viewed in the online issue, which is available at wileyonlinelibrary.com.]

hemostasis. Comparing with the number of studies appearing in the literature on the kinetics of crosslinking and/or properties of final particles, less attention has been paid to study the obtained particle size and size distribution of polysaccharide microspheres perhaps due to the complexity of the phenomena governing particle size in the inverse emulsion systems. As shown in Figure 7(a, b) for run orders 13 and 10, the CDMs had a polydispersity in size and were joined to others forming

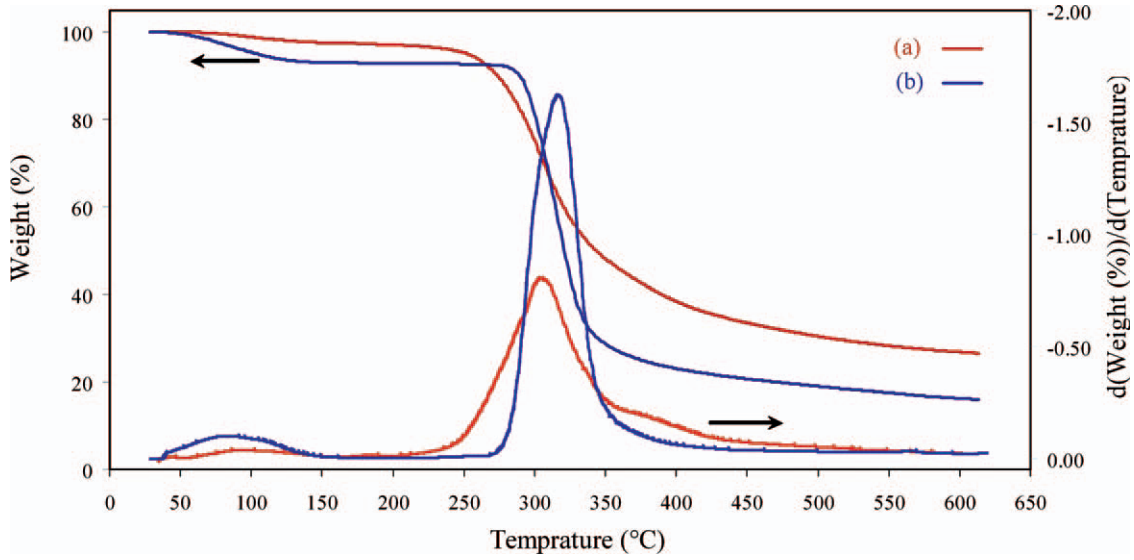

Figure 4. TGA and DTG thermograms of (a) crosslinked dextran microspheres and (b) initial dextran. [Color figure can be viewed in the online issue, which is available at wileyonlinelibrary.com.]

Table III. Results of Thermal Analysis Obtained for Initial Dextran and CDMs Under Nonoxidative Conditions

Sample	Humidity (W/W %)	Onset of thermal degradation (°C)	Maximum rate decomposition temperature (°C)	Final of thermal decomposition temperature (°C)	Residual mass at 600°C (W/W %)
Initial dextran	7.5	285	319	442	16.2
CDMs[a]	4	225	310	492	26.8

[a]Related to run order 10.

aggregates. In some experiments, wide particle-size distributions with UIs >1.5 calculated based on eq. (6) were obtained.

The observed polydispersity can be mainly attributed to the process parameters, e.g., flow pattern within the reactor or the emulsification method involved which are out of scope of this report. In details, when droplet breakage occurs by viscous shear forces, dextran solution droplets are first elongated into two fluid lumps separated by a liquid thread. Subsequently, the deformed droplet breaks into two almost equal size drops, corresponding to the fluid lumps, and a series of smaller droplets corresponding to the liquid thread. In regard with the amount of surfactant present in the solution, smaller droplets are formed via the breakage of droplets with higher volume. These smaller droplets are stable to the end of crosslinking reaction resulting in a wide particle-size distribution.[41,42]

Agglomeration was also observed in some extent, which is due to the induction of surface electrostatic charges during excessive drying of the CDMs and strong van der Waals forces among dextran molecules [Figure 7(a)].

Analysis of Experimental Design Findings

A full factorial DOE measures the response for every possible combination of factors and factor levels. These responses can be analyzed to provide information about every main and two-way interaction effects. A full factorial DOE is practical only when the investigated factors are less than five due to this fact that testing all combinations of factor levels are too time-consuming and expensive for higher number of factors.[43]

Equilibrium Swelling Ratio

Dextran concentration was found as the most effective term ($p < 0.05$) on the ESR of the resulting microspheres [Figure 8(a)]. F value was found to be 17.38, which imply that the model was significant. Increasing in dextran concentration in the aqueous internal phase resulted in droplets (reaction sites) which are rich in hydroxyl functional groups that play an important role in determining hydration pattern and crosslinking density of the polymer chains in the network. Rising in intermolecular entanglements due to increase in dextran concentration resists against relaxation and swelling of the chains In addition, CDMs are three-dimensionally crosslinked networks whose ESR depends on the crosslinking density. As the graphical analysis in Figure 9(a, 1; d, 1) reveals, the decrease in the ESR can be observed by both increased crosslinking ratio and dextran concentration. The reason for the observed decrease in swelling capacity is increasing in crosslinking which makes the network too dense. This dense structure can be described by decreased molecular weight between the crosslinks (M_c) and reduced mesh size (Table II) which restrict chain relaxation and decrease water uptake. The effect of input parameters on ESR is expressed as a polynomial equation as shown in Table IV [eq. (9)].

Thermal Decomposition Temperature

The most effective parameters affecting thermal stability of the CDMs were investigated by statistical analysis of T_f results. According to the results obtained from analysis of variance, dextran concentration, crosslinking ratio, and interaction between crosslinking ratio and surfactant concentration were found as

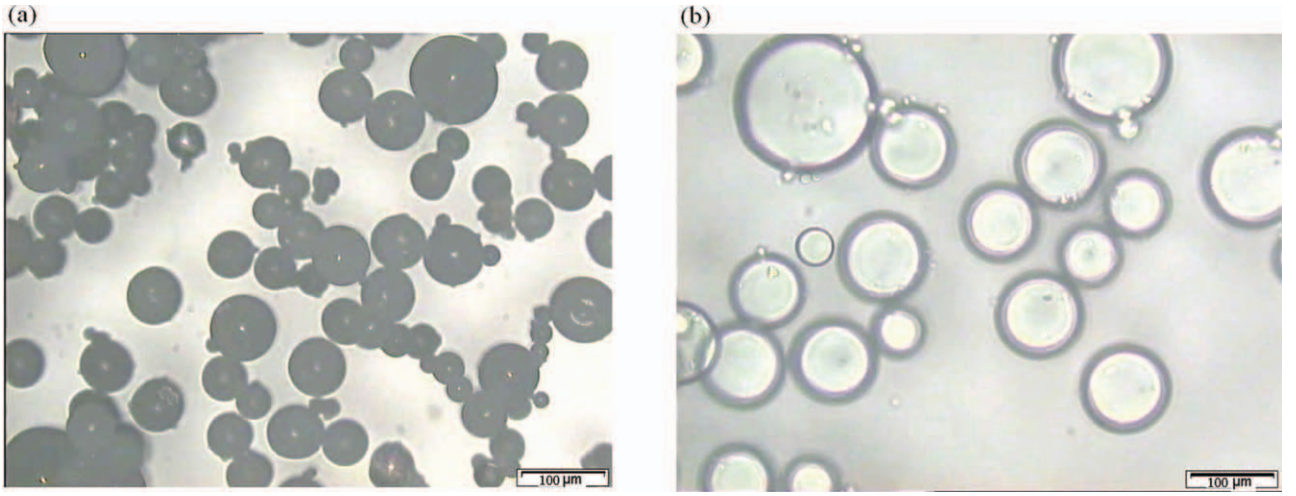

Figure 5. Optical micrographs of crosslinked dextran microspheres (run order 10 according to Table II) in dry (a) and swollen state in water (b). [Color figure can be viewed in the online issue, which is available at wileyonlinelibrary.com.]

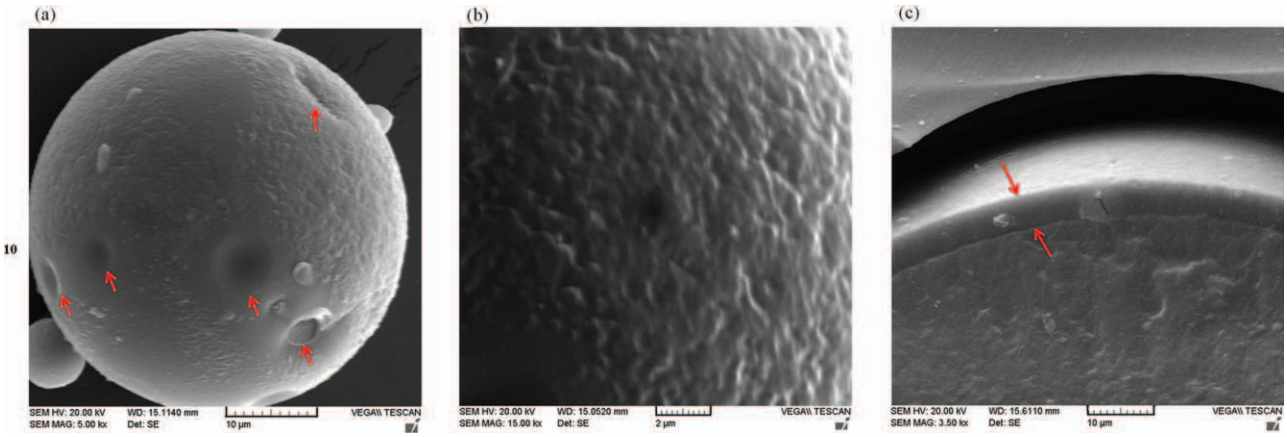

Figure 6. Typical scanning electron micrographs of microspheres showing (a) particles with moon-faced surface, (b) rough surface of microspheres, and (c) cross section of the particles (run order 10 according to Table II). [Color figure can be viewed in the online issue, which is available at wileyonlinelibrary.com.]

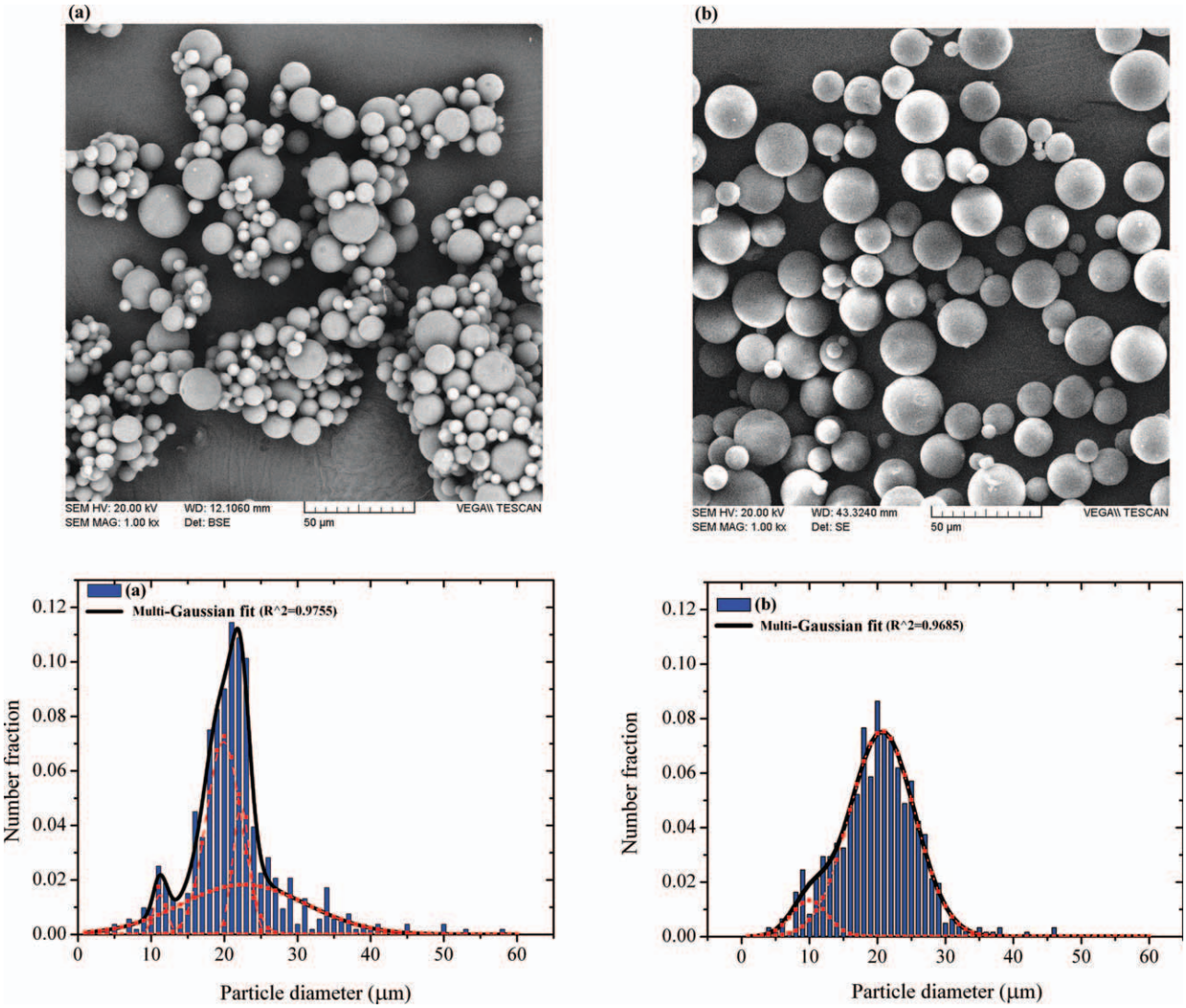

Figure 7. Backscattered micrograph and histogram of particle-size analysis with multi-Gaussian fitted model (a) for run order 13 according to Table II and secondary electron micrograph and the corresponding particle-size distribution histogram With multi-Gaussian fitted model (b) for run order 10. [Color figure can be viewed in the online issue, which is available at wileyonlinelibrary.com.]

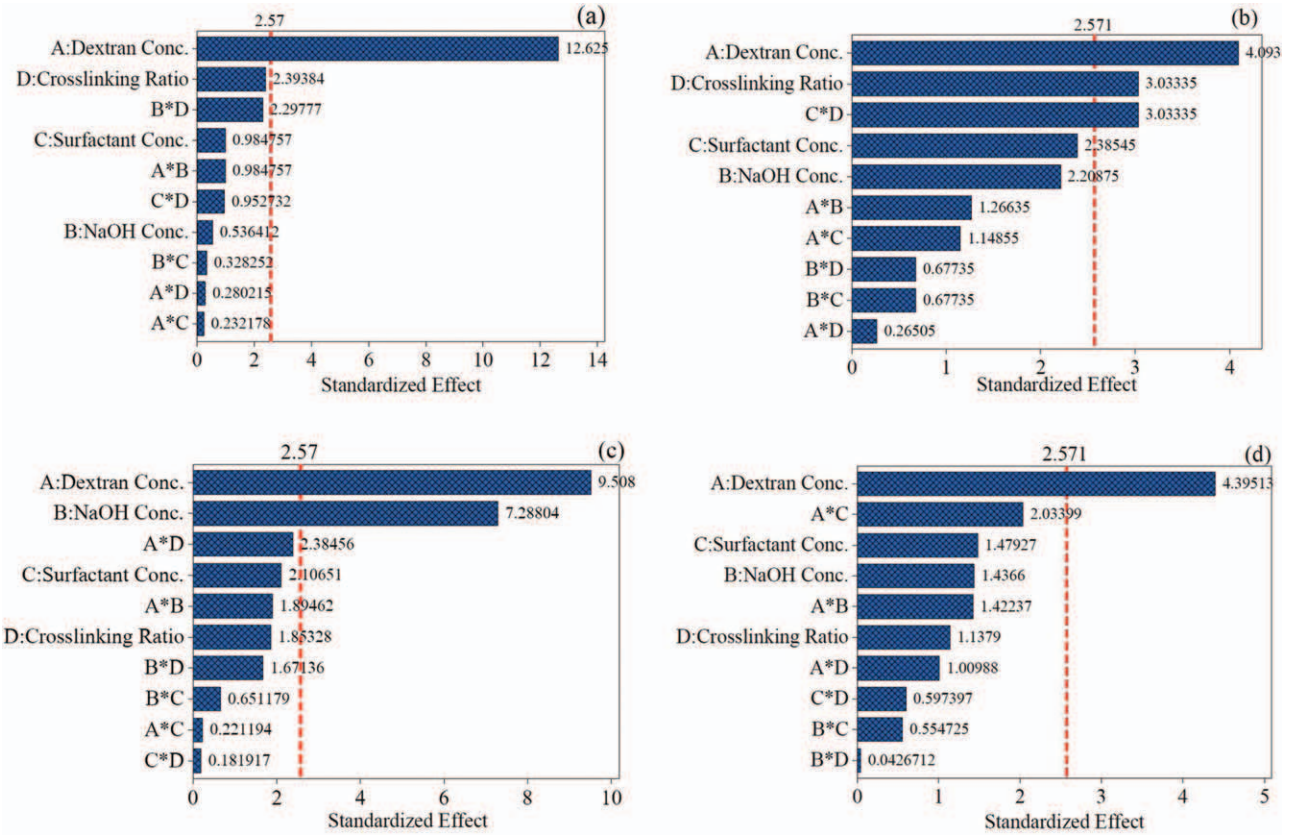

Figure 8. Standardized Pareto charts showing main effects of experimental parameters on the responses at the confidence limit of 95% for: (a) equilibrium swelling ratio, (b) final decomposition temperature, (c) mean particles size, and (d) uniformity index. [Color figure can be viewed in the online issue, which is available at wileyonlinelibrary.com.]

significant terms ($p < 0.05$) affecting final thermal decomposition temperatures of CDMs [Figure 8(b)]. As shown in Figure 9(a, 2; d, 2), increasing in the crosslinking reaction rate and/or crosslinking density of the microspheres via increasing in dextran solution concentration and crosslinking ratio causes an increase in T_f. It is obvious that the higher number of crosslinked bonds in the network has caused an increase in the final thermal stability of CDMs. Surfactant and NaOH concentrations were insignificant in this regard as shown in Figures 8(b) and 9(c, 2; b, 2). The relationship between thermal decomposition temperature and study variables is given in Table IV [eq. (10)].

Mean Particle Size and Uniformity Index

According to the model, dextran and NaOH concentrations in the aqueous phase have significant effects ($p < 0.05$) on the mean particle size of CDMs as shown in Figure 8(c). Based on marginal mean plots shown in Figure 9(a, 3), an increase in dextran solution concentration resulted in a corresponding increase in mean particle size of the microspheres. This significant increase is due to the increasing viscosity of the droplets as a consequence of increasing polymer concentration in solution. This increase is high enough to enhance the dispersed phase viscosity, which results in the reduced breakage rate of the droplets, and increases the emulsion droplet size and mean particle size of the final microspheres. The same mechanism can be proposed for the observed direct proportionality of NaOH concentration and mean particle size of the CDMs [Figure 9(b, 3)]. This is probably due to the increased polarization of hydroxyl functional groups on dextran backbone which in turn increases the solution viscosity. Considering the catalytic function of NaOH, higher rates can be expected for crosslinking reaction in the presence of higher NaOH concentrations which in turn causes higher rates for viscosity increment in the internal phase and lower breakage rate for droplets. The exact mechanism should be further explored. The regression-based model that describes the relationship between studied parameters and mean particle diameter is shown in Table IV [eq. (11)].

To eliminate the aggregates formed during the course of the crosslinking reaction, it was essential to add a minimal surfactant concentration of 0.5%. As shown in marginal mean plots [Figure 9(c, 3)], an increase in the surfactant concentration results in a slight but statistically insignificant reduction in the mean diameter of the microspheres which, shows that surfactant effect on the mean particle size is leveled off at high surfactant concentration regime. The rate of droplets breakup is a function of interfacial tension. Increasing the surfactant concentration decreases the interfacial tension between two phases; therefore, it facilitate break up of particles. Furthermore, drops with higher stabilizer coverage are less susceptible to coalescence after a collision.

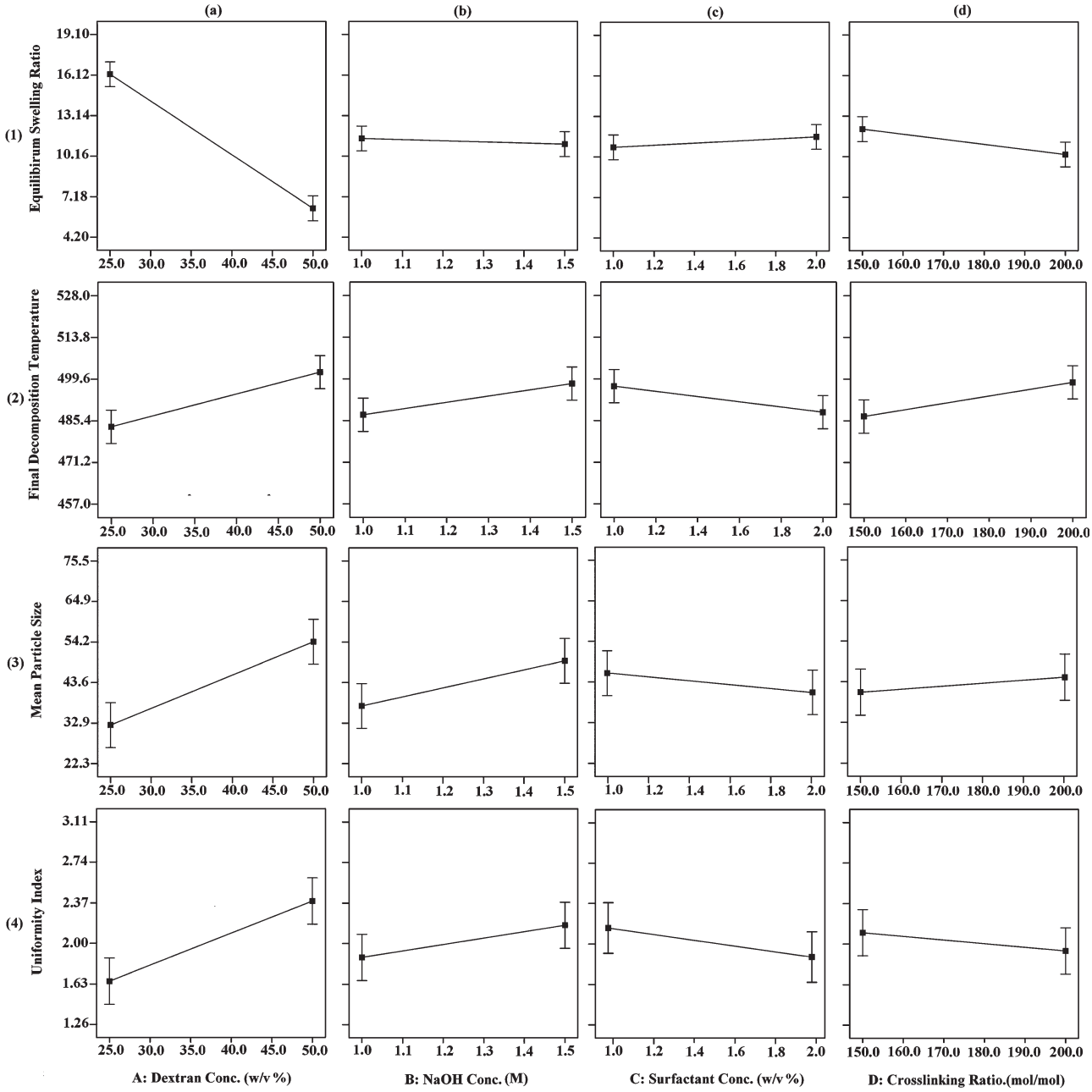

Figure 9. Plots of marginal means for (a) equilibrium swelling ratio, (b) final decomposition temperature, (c) mean particles size, and (d) uniformity.

Table IV. Regression Equations of the Fitted Models in Terms of Coded Values[a]

$$\text{Equilibrium swelling ratio} = 11.25 - 4.93 * A - 0.21 * B + 0.38 * C - 0.93 * D + 0.38 * A * B + 0.091 * A * C + 0.11 * A * D - 0.13 * B * C - 0.90 * B * D + 0.37 * C * D \quad (9)$$

$$\text{Final of thermal decomposition} = 493.31 + 8.69 * A + 4.69 * B - 5.06 * C + 6.44 * D - 2.69 * A * B - 2.44 * A * C + 0.56 * A * D - 1.44 * B * C - 1.44 * B * D - 6.44 * C * D \quad (10)$$

$$\text{Mean particle size} = 43.37 + 11.50 * A + 8.81 * B - 2.54 * C + 2.02 * D + 2.29 * A * B - 0.27 * A * C + 2.88 * A * D + 0.79 * B * C + 2.24 * B * D - 0.22 * C * D \quad (11)$$

$$\text{Uniformity index} = 2.04 + 0.39 * A + 0.13 * B - 0.13 * C - 0.10 * D + 0.12 * A * B - 0.18 * A * C - 0.089 * A * D + 0.049 * B * C - 3.750\text{E} - 003 * B * D + 0.052 * C * D \quad (12)$$

[a]Levels were coded as (−1) and (+1) for low and high levels, respectively.

In this study, no significant correlation was found between ECH concentration and mean particle size of CDMs; however, in contrast to a recent report,[38] the size of the CDMs was slightly decreased with decreasing in the crosslinker concentration.

According to Pareto chart obtained for UI [Figure 8(d)], dextran concentration is the most effective parameter that can directly affect the UI. According to the mechanism proposed for thorough breakage of an emulsion droplet,[44] the deformed droplet breaks into the two almost equal-size drops, corresponding to the fluid lumps and a series of smaller droplets corresponding to the liquid thread. Increase in internal phase viscosity results in increased viscoelastic properties of the dispersed phase. Therefore, droplets can elongate further by viscous shear forces and consequently more small droplets form on breakage of the droplets which in turn results to higher values of UI [Figure 9(a, 4)]. According to the results, it seems that increasing in the dispersed phase viscosity in any way, e.g. increasing in dextran and NaOH concentration may lead to broad CDMs particle-size distribution [Figure 9(b, 4)].

In this case, the surfactant was not able to favor the formation of small droplets during the emulsification process due to the lack of stability of the emulsions. More likely, it could form a film around the droplets, which prevented their coalescence possibly due to the Gibbs–Marangoni effect.[45] As shown in Figure 9(c, 3), UI was decreased and a narrow particle-size distribution was obtained by increasing in surfactant concentration, due to the reduced possibility of coalescence of the droplets during the formation of the microspheres.

CONCLUSIONS

Full factorial DOEs was used for systematic investigation of the effective parameters on the characteristics of dextran microspheres produced via an inverse emulsion-crosslinking method including mean particle size or swelling properties. Dextran and NaOH concentrations were found to be the most significant parameters determining mean particle size of the microspheres by increasing in internal phase viscosity or affecting the crosslinking reaction kinetics. Dextran concentrations and crosslinking ratio were also found as significant parameters for ESR upon their crucial role in determination of the finally produced microspheres structure. Promoting the crosslinking reaction caused a slight decrease in swelling capacity of the network due to more structural integrity provided thereof. The results indicate that the kinetics or processing conditions can be easily used to produce CDMs with different structural characteristics.

ACKNOWLEDGMENTS

The authors express their sincere gratitude to Iran Polymer and Petrochemical Institute (IPPI) for providing financial support to this research (contract grant number: 23711105).

REFERENCES

1. Saralidze, K.; Koole, L. H.; Knetsch, M. L. W. *Materials* **2010,** *3*, 3537.
2. Oh, J. K.; Lee, D. I.; Park, J. M. *Prog. Polym. Sci.* **2009,** *34*, 1261.
3. Topuz, F.; Okay, O. *React. Funct. Polym.* **2009,** *69*, 273.
4. Seyednejad, H.; Imani, M.; Jamieson, T.; Seifalian, A. M. *Br. J. Surg.* **2008,** *95*, 1197.
5. Freiberg, S.; Zhu, X. X. *Int. J. Pharm.* **2004,** *282*, 1.
6. Lopez, V. C.; Raghavan, S. L.; Snowden, M. J. *React. Funct. Polym.* **2004,** *58*, 175.
7. Petro, M.; Berek, D.; Novak, I. *React. Polym.* **1994,** *23*, 173.
8. Coviello, T.; Matricardi, P.; Marianecci, C.; Alhaique, F. J. *Controlled Release* **2007,** *119*, 5.
9. Slomkowski, S.; Basinska, T.; Miksa, B. *Polym. Adv. Technol.* **2002,** *13*, 906.
10. Heinze, T.; Liebert, T.; Heublein, B.; Hornig, S. *Adv. Polym. Sci.* **2006,** *205*, 199.
11. Oh, J. K.; Drumright, R.; Siegwart, D. J.; Matyjaszewski, K. *Prog. Polym. Sci.* **2008,** *33*, 448.
12. Li, M.; Rouaud, O.; Poncelet, D. *Int. J. Pharm.* **2008,** *363*, 26.
13. Zhang, F. J.; Cheng, G. X.; Ying, X. G. *React. Funct. Polym.* **2006,** *66*, 712.
14. Yao, R. S.; Gao, W. X.; Sun, J.; You, Y. H. *Chin. J. Polym. Sci.* **2005,** *23*, 401.
15. Zhang, J. G.; Xu, S. Q.; Kumacheva, E. J. *Am. Chem. Soc.* **2004,** *126*, 7908.
16. Arshady, R. *Polym. Eng. Sci.* **1989,** *29*, 1746.
17. Skiba, M.; Bounoure, F.; Barbot, C.; Arnaud, P. J. *Pharm. Pharm. Sci.* **2005,** *8*, 409.
18. Guner, A.; Akman, O.; Rzaev, Z. M. *O. React. Funct. Polym.* **2001,** *47*, 55.
19. Atyabi, F.; Manoochehri, S.; Moghadam, S. H.; Dinarvand, R. *Arch. Pharm. Res.* **2006,** *29*, 1179.
20. Pacek, A. W.; Ding, P.; Nienow, A. W. *Chem. Eng. Sci.* **2001,** *56*, 3247.
21. Bahukudumbi, P.; Carson, K. H.; Rice-Ficht, A. C.; Andrews, M. J. *J. Microencapsul.* **2004,** *21*, 787.
22. Berchane, N. S.; Jebrail, F. F.; Carson, K. H.; Rice-Ficht, A. C.; Andrews, M. J. *J. Microencapsul.* **2006,** *23*, 539.
23. Hamdi, G.; Ponchel, G.; Duchene, D. J. *Microencapsul.* **2001,** *18*, 373.
24. Flory, P. J.; Rehner, J., Jr. *J. Chem. Phys.* **1943,** *11*, 521.
25. Peppas, N. A.; Huang, Y.; Torres-Lugo, M.; Ward, J. H.; Zhang, J. *Annu. Rev. Biomed. Eng.* **2000,** *2*, 9.
26. Imren, D.; Gumusderelioglu, M.; Guner, A. *J. Appl. Polym. Sci.* **2006,** *102*, 4213.
27. de Jong, S. J.; van Eerdenbrugh, B.; van Nostrum, C. F.; Kettenes-van de Bosch, J. J.; Hennink, W. E. *J. Controlled Release* **2001,** *71*, 261.
28. Bo, J. *J. Appl. Polym. Sci.* **1992,** *46*, 783.
29. Peppas, N. A.; Hilt, J. Z.; Khademhosseini, A.; Langer, R. *Adv. Mater.* **2006,** *18*, 1345.
30. Canal, T.; Peppas, N. A. *J. Biomed. Mater. Res.* **1989,** *23*, 1183.

31. Dubey, R. R.; Parikh, R. H. *AAPS Pharm. Sci. Tech.* **2004,** *5*, 20.
32. Box, G. E. P.; Hunter, W. G.; Hunter, J. S. Statistics for experiments. An introduction to design, data analysis and-model building. New York: Wiley, **1978.**
33. Kartha, K. P. R.; Srivastava, H. C. *Starch Stärke* **1985,** *37*, 297.
34. Dragan, D.; Mihai, D.; Mocanu, G.; Carpov, A. *React. Funct. Polym.* **1997,** *34*, 79.
35. Spychaj, T.; Bartkowiak, A. *Polym. Adv. Technol.* **1998,** *9*, 138.
36. Ozdemir, C.; Colak, N.; Guner, A. J. *Appl. Polym. Sci.* **2007,** *105*, 1177.
37. Pariot, N.; Edwards-Levy, F.; Andry, M. C.; Levy, M. C. *Int. J. Pharm.* **2000,** *211*, 19.
38. Renard, E.; Sebille, B.; Barnathan, G.; Deratani, A. *Macromol. Symp.* **1997,** *1*, 229.
39. Hou, X.; Yang, J.; Tang, J.; Chen, X.; Wang, X.; Yao, K. *React. Funct. Polym.* **2006,** *66*, 1711.
40. Yuan, W. E.; Wu, F.; Geng, Y.; Xu, S. L.; Jin, T. *Int. J. Pharm.* **2006,** *339*, 76.
41. Jiugao, Y.; Jie, L. *Starch Stärke* **1994,** *46*, 252.
42. Maggioris, D.; Goulas, A.; Alexopoulos, A. H.; Chatzi, E. G.; Kiparissides, C. *Chem. Eng. Sci.* **2000,** *55*, 4611.
43. Motlekar, N.; Youan, B. B. *Drug. Des. Dev. Ther.* **2008,** *2*, 39.
44. Kotoulas, C.; Kiparissides, C. *Chem. Eng. Sci.* **2006,** *61*, 332.
45. Walstra, P. *Chem. Eng. Sci.* **1993,** *48*, 333.